

Sea Based Container Culture (SBCC) hydrodynamic design assessment for European lobsters (*Homarus gammarus*)

Peter Halswell^{*1}, Carly L. Daniels², Lars Johanning¹

¹ College of Engineering, Mathematics and Physical Sciences, University of Exeter, Exeter, UK.

² National Lobster Hatchery, Padstow, Cornwall, UK.

* Corresponding author. Tel.: 01326255751; E-mail: p.halswell@ex.ac.uk

Abstract

The presented work describes the hydrodynamic assessment studies of a much needed technical innovation of Sea Based Container Culture (SBCC) as part of a semi-intensive, passive aquaculture culture system for farming the European lobster (*Homarus gammarus*). Factors that are known to influence growth and survival rates were obtained from previous literature, including flow rate, wave energy and motion characteristics; these factors defined performance criteria for SBCC containers.

The internal flow velocities and external flow patterns for different SBCC container designs were measured and used to inform design decisions. Suitable graphical representations have been developed to assess SBCC containers on specific performance criteria. Oyster SBCC containers were found to provide stable motion characteristics but perform poorly against the lower velocity limit, indicating insufficient supply of Dissolved Oxygen (DO) to allow for optimal growth of European lobsters. Internal flow velocities were also measured on unfouled and fouled SBCC containers; results showed SBCC 2 would not provide enough DO with 66% biofouling coverage (66% biofouling replicates one year deployment) and triggered a redesign. SBCC 1 at 90° yaw angle of attack demonstrated all round good performance against upper and lower velocity limits and motion characteristics; thus showed greatest promise for cultivation of European Lobster.

Keywords

European lobster
Aquaculture
Hydrodynamic
Design assessment
Growth
Survival

Abbreviations

AoA	Angle of Attack
ADV	Acoustic Doppler Velocimeter
DO	Dissolved Oxygen
SBCC	Sea Based Container Culture

Highlights

- Hydrodynamic design assessment of novel sea based container culture (SBCC) containers for European lobsters.
- Performance criteria for growth and survival include upper and lower velocity limits and motion severity.
- Assessment of internal velocity against velocity limits demonstrated SBCC 1 at 90° angle of attack provide best conditions.
- Assessment of motion severity showed a circular container (Oyster SBCC) provides stable motion characteristics.
- Normalised comparison provided fair comparison of performance criteria.

1 Introduction

The world's population is forecast to rise by one third between 2009 and 2050 (DESA, U.N., 2013). Due to limited agricultural land and growing pressure on exploited marine livestock, aquaculture could increase productivity and contribute to global food security by providing a sustainable food source to feed the growing population. Between 2006 and 2011, captured fishery production increased by only 0.4%; whereas, aquaculture production grew by 34.5% (Mathiesen, 2012). Many species present potential as candidates for aquaculture that are currently unexploited in the sector, a promising candidate being the European Lobster (*Homarus gammarus*) for the following reasons. The demand for European lobster currently exceeds supply, resulting in high prices across global markets (Drengstig and Bergheim, 2013). Supply is limited to approximately 5,000 tonnes per year coming from capture fisheries based mostly in the UK and Ireland (<http://www.fao.org/fishery/species/2648/en>), though the majority of this is exported. Currently much of the market deficit for lobsters in Europe is met via the import of live American lobster (*Homarus americanus*) (Davies et al., 2014), though there are growing concerns over the potential invasiveness of escapees and inadvertent releases to damage native ecosystems (van der Meeren et al., 2000, 2010; Jørstad et al., 2007; Stebbing et al., 2012).

Trials in Norway utilising Recirculating Aquaculture Systems (RAS) have recently illustrated the potential for farming lobster to market size (Drengstig and Bergheim, 2013), but there is still a lack of appropriate technological development in RAS design, married to inappropriate economies of scale. In RAS systems difficulties can arise from; maintaining required water quality (temperature, salinity, ammonia and dissolved oxygen), feeding necessities, high capital investment and the labour intensive nature of such systems (Drengstig and Bergheim, 2013). Due to the cannibalistic nature and slow growth rates exhibited by the species, the lobster demands the use of a rearing system that has; individual compartments, is relatively inexpensive to construct and operate, is simple and inexpensive to maintain, is based on non-anthropogenic food supply, is self-cleaning, allows for sufficient feed and water exchange from naturally occurring sources, enables high stock density production while ensuring optimal growth and survival, and permitting easy access to livestock for inspection (modified from Drengstig and Bergheim, 2013). A potentially viable solution is a Sea Based Container Culture (SBCC) system because water quality and feed is supplied naturally by the sea and, capital investment and labour is minimal in comparison to land based techniques (Uglem et al., 2006; Benavente et al., 2010; Daniels et al., 2015). The feasibility of lobster SBCC systems has been tested using a variety of containers including one originally designed for rearing oyster sprat (Fig. 1; manufactured by Pelegrin Y Manresa, S.L., Alicante, Spain) with good success (Uglem et al., 2006; Benavente et al., 2010; Browne et al., 2011; Daniels et al., 2015). These preliminary studies have established: 1) low energy costs, 2) zero feed costs 3) fixed unit cost of production (compared to an escalating cost against time in land based culture) and 4) good short term survival and growth rates. SBCC systems therefore hold the potential to deliver a low carbon system for sustainable aquaculture, providing a valuable human protein source at minimal unit cost.

A biological literature review, performed prior to this study, identified critical parameters for the growth of the European lobster. The three critical parameters related to the hydrodynamic performance of SBCC systems include (though are not limited to); *flow rate*, *wave energy* and *motion characteristics* (Burton, 2003; Drengstig and Bergheim, 2013; Galparsoro et al., 2009; Howard and Nunny, 1983; Smith, 1999; Uglem et al., 2006). Flow rate is important in providing sufficient oxygen and food as well as removing waste to ensure optimal lobster growth is obtained (Drengstig and Bergheim (2013), Uglem et al., 2006 and Burton. 2003)). Flow rates previously reported to be successful for rearing lobster range from 4 L/min (Beal et al., 2002) to 100 L/min (Drengstig and Bergheim, 2013). Wave energy can influence feeding behaviour and growth as well as causing physical damage and potentially mortality (Galparsoro et al., 2009; Howard and Nunny, 1983; Smith, 1999). Wave energy sources resulting in velocities in excess of 250 mm/s can inhibit food gathering activity of lobsters and hence should be minimised (Galparsoro et al., 2009). Lobsters also experience stress, or exhibit reduce feeding behaviour if they live in a space that experiences dynamic motion (Galparsoro et al., 2009; Smith, 1999).

This paper aims to compare hydrodynamic properties of SBCC designs, to identify the most suitable container for rearing *H. gammarus* based on assessments below:

- 1a) Measure the internal flow patterns at different flow velocities, angles of attack (AoA) and percentage of biofouling.
- 1b) Development of a graphical methodology to inform best design configuration, presenting internal flow patterns and, upper and lower velocity limits.
- 2a) Visualise and assess motion characteristics and severity (only allowing 2D motion; X- and Y-axis) caused by external flow velocities.
- 2b) Visualise external flow patterns (using dye-tracing method) and identify causes of motion characteristics (visualised in step 2a).
- 2c) Analyse and rate the SBCC containers based on their motion characteristics towards potential impact of lobster development (from 2a) and recommendation methods to reduce excessive SBCC container motion (from 2b).

2 Materials and Methods

The hydrodynamic performance of scaled SBCC containers, designed specifically for lobsters, was evaluated in the current flume based at the University of Exeter, Penryn campus, Cornwall, UK. Scale models were moored in the current flume on a specially designed model-bracket and end plates (Section 2.1). Internal velocities were measured using Acoustic Doppler Velocimetry (ADV) fitted to a traverse system to automate the measurement of flow conditions (Section 2.1.4). 2-D motion characteristics of SBCC containers were visualised by allowing freely rotation in X- and Y-axis coordinates whilst recording the motions (Section 2.1.5). To assess the cause of motion the external flow patterns were visualised using a dye-tracing method (Rathakrishnan, 2007; Section 2.1.5).

2.1 Experimental configuration

2.1.1 Hydrodynamic facility

A hydrodynamic test facility (Fig. 2) comprising of a recirculating water tank (called a current flume) providing controlled input flow velocities was used to measure internal velocities and visualisation external flow patterns. The test section (Fig. 2b) was of 2 m long, 0.6 m wide and 0.6 m deep, with a maximum input flow velocity of 1 m/s. A near laminar flow condition was achieved at the test section by passing the inlet flow through a honeycomb flow straightener which removed eddies greater than 10 mm. The water depth was checked at the start of each day. The flume required three minutes settling time for the input velocity to reach a quasi-steady state.

SBCC models were attached to the current flume using a custom built model-bracket (Fig. 3), specially designed to minimise hydrodynamic effects on flow conditions and deflection due to fluid loading. At sea, SBCC container would typically be stacked during deployment (Fig. 1a) and thus experience 2D flow conditions over the majority of stack height. To achieve such 2D flow conditions on a single SBCC container during the present study, end plates (Fig. 3) were used to control vertical flow velocities (Rathakrishnan, 2007). Endplates were not used to study the motion characteristics of SBCC containers because end plates restrict motion; as such during these experiments the container experienced 3D flow conditions.

2.1.2 Scale-models of SBCC containers

Physical scale models of four SBCC containers (Oyster and three novel designs – novel designs not disclosed due to confidentiality) were 3D printing from ABS plastic, see Fig. 4. The chosen scaling ratio was 1:1.6.

2.1.3 Biofouling

Field studies showed a one year deployment reduced the area of open mesh by approximately 68%. Increased biofouling will reduce water flow into the containers reducing the dissolved oxygen (DO) availability for lobsters with potential detrimental effects. Therefore, the effect of biofouling on DO availability (lower velocity limit) is the primary concern. The effect of biofouling on flow was simulated using non-soluble, engineering putty to block the columns of mesh on the scales containers (Fig. 5). Biofouling tests were undertaken on SBCC 1 and 2. The percentage of biofouling ($\%_{bio}$) was calculated using equation (1) where A_{mesh} is the area of open mesh (m^2) and A_{bio} is the area of open mesh (m^2) covered by biofouling.

$$\%_{bio} = 100(A_{bio}/A_{mesh}) \quad (1)$$

The roughness value (k) was calculated using equation (2) where h_p is derived from the putty height (mm) and D is the characteristic container length (mm).

$$k = h_p/D \quad (2)$$

Table 1 provides percentage of biofouling and roughness values for SBCC 1 and 2. The putty heights were comparable between SBCC 1 and 2, and the standard deviation was a maximum of 27% of putty height.

Table 1

Roughness characteristics of biofouling (model-scale dimensions).

SBCC	Biofouling (%)	h_p	St.Dev of h_p	D	k
SBCC 1	33	0.630	0.126	215	2.93×10^{-3}
	66	0.864	0.135	215	4.02×10^{-3}
SBCC 2	33	0.538	0.143	334	1.61×10^{-3}
	66	0.740	0.105	334	2.21×10^{-3}

2.1.4 Internal velocities measurements

Internal velocities were measured using an ADV (Vectrino-Profiler, Nortek AS., Rud, Norway), see Fig. 6. The ADV, had an accuracy of $\pm(1 \text{ mm/s} + 0.5\% \text{ of measurement value})$ and sampling frequency of 100 Hz and provided an accurate, semi-intrusive method to measure velocity. Hollow glass spheres (manufactured by Potter Industries Inc. - product number 110P8, Yorkshire, UK) were used as a seeding particle in the water to reflect acoustic measurement signals. The ADV was fitted to a traverse system, on the outside of the upper end plate (Fig. 3), with a spatial resolution of $\pm 0.05 \text{ mm}$ (Nortek Vectrino Profiler, 2015) to automate the measurement of thousands of individual points (Table 3).

A defined pattern (aperture) was cut into the SBCC container lid to allow internal velocity measurements within the SBCC containers. The aperture was shaped to match the Vectrino-Profiler probe head, a cross shaped, with a height and width of 70 mm and a thickness of 6 mm. A sliding lid was developed to allow a single lid with a single aperture to be adjusted accordingly for multiple measurements by translating the sliding lid and ADV simultaneously.

2.1.5 External flow visualisation

During motion characterisation, SBCC containers were attached to the model bracket allowing only a free rotation in the yaw motion. This provided an idealised 1D rotational motion (yaw) with restrictions to the remaining rotational motion (pitch and roll), and all three transverse motions (heave, surge and sway). A video camera (HD HC-V50, Panasonic) with 10 megapixel resolution recorded the yaw motion. A geometrically correct lid was implemented instead of the sliding lid as an aperture was superfluous for flow visualisation.

External flow pattern visualisation was conducted using a dye-tracing method to visualise the flow phenomenon (Rathakrishnan, 2007). Dye-tracing involved manually injecting dye (ink) into the fluid flow, through a long, narrow pipette and a syringe, and recording the streamline paths. The outer diameter of the pipette was 7 mm and the inner nozzle diameter was 1 mm. The dye release point was horizontally located at the leading edge of the end plates and vertically located midway between the two end plates. The dye was released at 0 mm and 50 mm from the longitudinal centreline. Approximately 2 mL of dye was used per visualisation.

2.2 Performance criteria

Performance criterial identified from critical growth and survival parameters to assess the suitability of SBCC designs are described in the following sections.

2.2.1 Lower velocity limit

Flow rate (L/min) was converted into velocity (m/s) to provide a lower velocity design limit that was geometrically precise parameter (whereas flow rate is an average flow through the system) and is appropriate for dimensionless analysis. A lower velocity limit of 4.1 mm/s was derived from the time required for lobsters to reduce the Dissolved Oxygen (DO) inside an internal container during all life stages based on refreshment requirements. The lower velocity limit (u_{lower}) was calculated from equation (3):

$$u_{lower} = \frac{L}{t} \quad (3)$$

where the continuous (i.e. no empty space between SBCC containers because no DO is consumed) length of the SBCC array¹ (L) was 147 m and the time constant of available DO (t) was calculated from equation (4):

$$t = \frac{V(DO_{sea} - DO_{lobster})}{C} \quad (4)$$

where the volume of the SBCC internal container (V) was 1.559 L, the lowest DO levels in sea water (DO_{sea}) was 7.54 mg/L (data requested from Par Surface boil site obtained by the Environment Agency between 2013-2015), the lowest acceptable DO levels for optimal growth ($DO_{lobster}$) was 6.4 mg/L (Drengstig and Bergheim, 2013) and the maximum DO consumption rate (C) of a 150 g lobster was 5×10^{-5} mg/s (Hamel, 2006).

The lower velocity limit compares to the mean and median X-axis flow through the SBCC containers because the fresh water supply of DO is only in the X-axis. The lower velocity limit is dependent on a number of parameter (levels of DO in sea, size of lobster, size of SBCC array, etc.). Herein it's considered a constant for comparison between SBCC systems; however, its use should be carefully considered for other applications.

2.2.2 Upper velocity limit

The observation by Howard and Nunny that orbital velocities exceeding 250 mm/s affecting feeding behaviour and stress of lobsters was applied in a direct relation and sets an upper velocity limit. In addition to the mean flow velocity obtained from instantaneous velocity measurements the turbulent fluctuations was also considered using the Prandtl mixing-length hypothesis (Fox, 1977). For this, the instantaneous velocity (U) was calculated by combining steady velocity (u) and turbulent fluctuation (u') given equation (5):

$$U = u + u' \quad (5)$$

The upper velocity limit relates to velocity magnitude (i.e. maximum velocity regardless of direction) because the effect of high velocities on feeding behaviour and stress is regardless of direction.

¹ 147 m was a constant, arbitrary number used for comparison of SBCC systems. Discussions with a mussel aquaculture farmer suggested that an initial full-scale deployment plan was a 200 m farm with a stack of SBCC containers every metre. The largest SBCC system tested was 0.735 m diameter so the continuous length was 147 m ($L = 200 \times 0.735$).

2.2.3 Motion characterisation

The magnitude of dynamic motion required to induce stress or reduce feeding behaviour has not been quantified, thus a limit cannot be defined. Instead, the dynamic motion must be minimised as much as practically possible.

2.3 Experimental procedure

2.3.1 Procedures for internal velocities

Flow velocities applied for this study are based on full scale conditions obtained from a field demonstration site near Falmouth, Cornwall, UK; the Falmouth Bay Test site (FaBTest), with a maximum velocity of 0.75 m/s. Therefore, the full-scale input velocities for the flume tests were: 0.1, 0.3, 0.5 and 0.7 m/s. To study the influence of the flow at various AoA, inline (0°) and transverse (90°) alignments of SBCC containers to flow direction were studied, as well as a 36° for Oyster SBCC. Three percentages of biofouling were studied: 0, 33 and 66%. A summary of test parameters have been presented in Table 2.

Table 2

Test parameters for internal velocity measurements.

SBCC	Full-scale velocities (m/s)	AoA ($^\circ$)	Biofouling (%)
Oyster	0.1, 0.3 & 0.5	0 & 36	0
SBCC 1	0.1, 0.3, 0.5 & 0.7	0 & 90	0, 33 & 66
SBCC 2	0.1, 0.3, 0.5 & 0.7	0 & 90	0, 33 & 66
SBCC 3	0.1, 0.3, 0.5 & 0.7	0	0

The following procedures were used for the internal velocity measurements of one individual compartment (Fig. 1). The procedure was repeated for the next individual compartment.

1. Align SBCC model using a right-angle set square on glass side of flume.
2. Vertically align Vectrino-Profilers with SBCC base using bottom check function.
3. Horizontally align Vectrino-Profilers using a right-angle set square on glass side of flume.
4. Start flume at required speed and allow 3 minutes settling time.
5. Record 6000 data points for each measurement location (60 s at 100 Hz)
6. Move to new location.
7. Repeat steps 5 and 6 until all measurements were made inside one individual compartment.

The maximum spatial resolution of measurement locations was set as smaller than the length of juvenile lobsters and the spatial resolution was approximately 10 mm in X- and Y-axis and 1 mm in Z-axis. The measurement locations of Oyster SBCC at 0° and 36° AoA are shown in Fig. 7, novel designs not shown for confidentiality reasons. The number of measurement locations per SBCC container is summarised in Table 3.

Table 3

Number of internal measurements location per SBCC container

SBCC	Number of measurement locations
Oyster	11,400 (0° and 36° AoA)
SBCC 1	6,200 (0° AoA) and 6,450 (90° AoA)
SBCC 2	10,300 (0° AoA) and 5,200 (90° AoA)
SBCC 3	7,100 (0° AoA)

2.3.2 Procedures for motion characterisation

Test parameters for motion characterisation (Table 4) were input velocity and AoA (SBCC 1 can be moored in two orientations so two AoA were tested). The motion was recorded for three minutes. Test parameters for external flow pattern visualisation were the same as the internal velocity measurements (Table 2); tests were repeated with and without lids.

Table 4

Test parameters for motion characterisation.

SBCC	Input velocities (m/s)	Mooring points
Oyster	0.1, 0.3 and 0.5	1
SBCC 1	0.1, 0.3, 0.5 and 0.7	2 (0° & 90° AoA)
SBCC 2	0.1, 0.3, 0.5 and 0.7	1
SBCC 3	0.1, 0.3, 0.5 and 0.7	1

2.4 Post processing

Post processing was conducted to remove outliers, convert model-scale velocities to full-scale velocities and generate standard and cumulative histograms as design graphs. There were two sources to corrupt data; vibrations from the traverse system and interference from the container floor. Vibrations from the traverse system occurred due to sudden stopping after a traverse movement, so the first two seconds of every location were removed. Interference from the container floor occurred from locking tabs associated with internal dividers that protruded from the container and reflected the acoustic signal (from the Vectrino-Profiler) and caused a false value. The Signal to Noise Ratio (SNR) of the reflected signals off the tabs was significantly higher than the SNR of reflected signals off seeding particles, thus data were disqualified if the SNR was above 45 dB.

Full-scale velocities were calculated from model-scale velocities using dimensionless analysis and Reynolds number constituted the dimensionless parameter (equation (6)) where u is velocity (m/s), L is length (m) and ν is kinematic viscosity (m^2/s). The kinematic viscosity depends on both temperature and salinity, and the International Towing Tank Conference - Recommended procedures: 7.5-02-01-03 provided reference values. The average sea temperature was chosen to be 10°C for full-scale and the current flume temperature was measured using the Vectrino-Profiler at 100 Hz.

$$\frac{u_1 L_1}{\nu_1} = \frac{u_2 L_2}{\nu_2} \quad (6)$$

2.5 Calibration validation

Calibration validation methods were used to assess the accuracy of experimental experiment. The Vectrino-Profiler is reported by Nortek AS to have an accuracy of $\pm(1 \text{ mm/s} + 0.5\%$ of measurement value); however, the accuracy the Vectrino-Profiler was validated in-house and was shown to be closer to $\pm 2 \text{ mm/s}$ depending sample cell within the profile; the centre sample cells of the profile had a greater accuracy than the edge sample cells. The accuracy of the Vectrino-Profiler was measured by moving the Vectrino-Profiler through quiescent water using the traverse system so that the only flow velocities measured were cause by the movement of the traverse system. The Vectrino-Profiler also has a self-induced error called acoustic streaming. Acoustic streaming can generate steady fluid flow velocities between 0.05 cm/s and 2 cm/s in the Z-axis (Poindexter, 2011). In-house validation showed the effect of acoustic streaming is negligible when the cross-flow velocities were above 6 mm/s with a velocity range of 0.1 m/s . Therefore, all measured velocities under 6 mm/s were highlighted during post processing and it was found that less than 0.5% of the measured velocities magnitudes and RMS turbulence fluctuations were less than 6 mm/s only with 0.1 m/s input velocity. Upon closer inspection, the velocities below 6 mm/s were partly caused by interference from the SBCC container floor. Therefore, acoustic streaming only affected approximately 0.25% of measurements when the input velocity was 0.1 m/s and it was not accounted for in post processing methods.

The spatial resolutions of the traverse system stepper motors were $\pm 0.05 \text{ mm}$; however, this did not consider the repeatability, which was reduced by flexibility within the traverse structure in the X- and Y-axis. The accuracy of the traverse system including flexibility was measured to be $\pm 2 \text{ mm}$ and $\pm 1 \text{ mm}$ in the X- and Y- axis, respectively. The accuracy in the Z-axis due to a marginally unlevelled traverse system was shown to be less than $\pm 1 \text{ mm}$ over the entire $2 \text{ m} \times 0.6 \text{ m}$ plane.

A detailed calibration was conducted to study the flow conditions within the flume with model-bracket. The outcomes from flume characterisation showed a linear relationship between the motor power and mean X-axis velocity (Fig. 8). The turbulence velocities were also measured during the flume characterisation and it was concluded that the RMS turbulence fluctuation velocities (u'_{rms}) range between $1/12$ and $1/20$ of the mean X-axis velocity (Fig. 9), where RMS turbulence fluctuation is expressed using equation (7).

$$u'_{rms} = \sqrt{(U - u)^2} \quad (7)$$

3 Results

All values (geometry and velocity) are reported at full-scale, unless otherwise stated.

3.1 Oyster SBCC

3.1.1 Internal velocities

The internal velocity distribution is pictorially display in two manners: 3D velocity vectors (Fig. 10), and horizontal 2D plane of velocity magnitude and RMS turbulent fluctuation mid-

height from container floor (Fig. 11). There were observable differences between the upstream and downstream containers of Oyster SBCC at 0.1 m/s velocity and 0° AoA (Fig. 10a). The upstream containers comprised of high flow velocities near the centreline (between $Y < -110$ mm and $Y > 100$ mm of Fig. 11a) of the SBCC container with lower velocities at the edges. The downstream containers consist of lower velocities than the upstream containers, where the flow velocity distribution was generally more disperse, except the upper aft edge. The aft edge also experienced the highest turbulent fluctuations (Fig. 11a). The velocity distribution at 36° AoA (Fig. 10b and Fig. 11b) had less observable variation between the 4 internal containers than at 0° AoA (Fig. 10a and Fig. 11a); however, each internal container exhibited an area of high flow velocity with a matching area of high turbulence.

The cumulative histogram of internal velocity distribution (Fig. 12) for the Oyster SBCC shows that the velocities were generally higher at 36° AoA than 0° AoA, for all input velocities. The velocity distribution conforms to a near normal distribution at 0° AoA; however, 36° AoA distribution intersects the 0° AoA distribution indicating there are two regions of separate flow patterns.

3.1.2 Motion characteristics

Oyster SBCC had a stable yaw AoA at all input flow velocities (meaning that the yaw motion did not oscillate once the stable AoA was reached). The yaw AoA aligned in a way that the divide between the internal containers was 45° to the input flow direction (Fig. 13).

Dye-tracing confirmed that the external flow patterns of Oyster SBCC are comparable to a quasi-2D cylinder, showing a turbulent wake (Fig. 14c). The horizontal streamline paths flow around the superstructure and the separation point was approximately at the maximum width (Fig. 14d). Dye-tracing also reinforced the internal velocity measurements using the Vectrino-Profilers, as high internal velocities were found along the centreline of the upstream containers (Fig. 14b), and velocities were more dispersed in the downstream containers (Fig. 14d).

3.2 Comparison per performance criteria

3.2.1 Lower velocity limit

The percentage of measurement points against the X-axis velocities cumulative histogram (Fig. 15) shows that a considerable percentage (~35-55%) of measurement points inside Oyster SBCC and SBCC 2 were below the lower velocity limit (4.1 mm/s). In particular, 54% of Oyster SBCC measurement points at 0° AoA were below the lower velocity limit; therefore, the median X-axis velocity was less than 4.1 mm/s. SBCC 1 and 3 have smaller percentage of measurement points (<5%) below the lower velocity limit.

Cumulative histograms provide a value equivalent to the median X-axis velocity; although, the mean velocity also quantifies the lower velocity limit. The mean X-axis velocity against input velocity (Fig. 16) shows that a linear relationship can be assumed. A minimum input velocity to generate mean X-axis flow velocities greater than the lower velocity limit can be extracted, which provides a minimum operating tidal velocity for each SBCC container (Table 5). It is predicted that SBCC 1 and 3 require between 14 mm/s and 17 mm/s to

generate mean X-axis internal velocity above 4.1 mm/s; whereas Oyster SBCC required between 47 mm/s and 53 mm/s (Table 5). The linear assumption is limited to turbulent flow and the relationship will transform during the laminar-turbulent transition. This linear assumption limit was predicted using the Reynold's number and the critical speed that the Reynold's number falls below 2000 is 9 mm/s, where kinematic viscosity = $1 \times 10^{-6} \text{ m}^2/\text{s}$ and $L = 215 \text{ mm}$ (smallest characteristic length of SBCC scale-models). A Reynold's number of 2000 is commonly regarded at the transition between laminar and turbulent flow. Thus the linear assumption is close to its limitation but still provides another performance comparison of SBCC containers.

Table 5

Minimum input velocity required to generate mean X-axis velocity above lower velocity limit.

SBCC	Minimum input velocity (mm/s)
Oyster - AoA 0	47
Oyster - AoA 90	53
SBCC 1 - AoA 0	14
SBCC 1 - AoA 90	17
SBCC 2 - AoA 0	37
SBCC 2 - AoA 90	26
SBCC 3	15

3.2.2 Upper velocity limit

The percentage of measurement points against the X- and Y-axis velocity magnitude plus RMS turbulent fluctuation cumulative histogram (Fig. 17) compares the upper velocity limit (250 mm/s) performance of SBCC containers regardless of flow direction. At 0.5 m/s input velocity, Oyster SBCC had the smallest percentage of measurement points (0.25%) over the upper limit and SBCC 3 has the largest percentage of measurement locations (34%) over the upper limit. SBCC 1 and 2 provide intermediate performance. Performance comparisons between SBCC containers were observably similar at other input velocities (0.3 m/s and 0.7 m/s).

3.2.3 Biofouling

Biofouling experiments were performed at 0.3 m/s input velocity because a linear assumption between input velocity and mean X-axis internal velocity was demonstrated (Section 3.2.1; Fig. 16). The effect of biofouling on X-axis velocity is shown in Fig. 18 and Fig. 19. Biofouling on SBCC 1 at 90° AoA increased the percentage of measurement points below the lower velocity limit from 1.5% at 0% biofouling to 8.7% at 66% biofouling (Fig. 18). Biofouling on SBCC 2 at 0° AoA was shown to increase the percentage of measurement points below the lower velocity limit; from 26% at 0% biofouling to 69% at 66% biofouling (Fig. 19).

3.2.4 Motion characteristics

The yaw motion characterisation showed that Oyster SBCC and SBCC 2 had stable yaw AoA resulting in the least severe motion (motion severity 1); whereas, SBCC 1 and 3 were unstable. SBCC 3 exhibited the largest amplitude motion (motion severity 4) leading to the harshest motion (Table 6). SBCC 1 performed intermediately (motion severity 2/3) and with the motion severity varying between the two AoA (Table 6).

Table 6

Quantification of motion characteristics for SBCC containers.

	Oyster	SBCC 1		SBCC 2	SBCC 3
		AoA 0°	AoA 90°		
AoA	45°	-	-	90°	-
Un/stable	Stable	Unstable	Unstable	Stable	Unstable
Magnitude of rotation (°)	0	8.5	2.5	0	11
Motion severity (1=best, 4=worst)	1	3	2	1	4

4 Discussion

4.1 Lower velocity limit

The median X-axis velocities (Fig. 15) of Oyster SBCC and SBCC 2 were below the lower velocity limit, which indicates these containers did not provide enough DO for optimal growth at 0.1 m/s input velocity. Oyster SBCC and SBCC 2 required the highest input velocities (ranging from 26 mm/s to 53 mm/s; Table 5) to supply sufficient DO, reinforcing the conclusion from the median X-axis velocities. Furthermore, the internal velocity vector distribution of Oyster SBCC (Fig. 11) did show regions of back flow leading to recirculated water. Generally, Oyster SBCC and SBCC 2 required design improvements to enhance the X-axis flow at all AoA. On the other hand, SBCC 1 and 3 were shown to have good mean and median X-axis velocities compared to the lower velocity limit and should provide sufficient DO for optimal growth. The fundamental difference between Oyster SBCC and SBCC 2, and SBCC 1 and 3 was the outline shapes, which were circular and streamlined respectively. A circular SBCC container did not develop suitable X-axis flow to provide fresh water with high levels of DO and food.

4.2 Upper velocity limit

Oyster SBCC had the smallest percentage of measurement points over the upper limit; this suggests that feeding behaviours and stress will not be affected at high input velocity. In contrast, SBCC 3 had the largest percentage of measurement locations over the upper limit, which implies lobsters may become stressed and reduce their feeding rates at higher input velocity (i.e. 0.5 and 0.7 m/s). However, the distribution of high velocities within the SBCC containers must be considered because lobsters can avoid harmful, high flow velocities by positioning themselves in regions of lower velocities. Fig. 20 shows the measurements that exceeded the upper velocity limit of SBCC 2 (which has six distinguishable compartments;

no more confidentially sensitive information can be disclosed) at 0.7 m/s input velocity were primarily located in the upstream containers; therefore, lobsters in upstream containers could not avoid the unfavourable, high velocities. This approach was applied to the other SBCC containers. SBCC 3 showed high velocities were scattered within low velocities and there was no region of low velocity for a lobster to evade into. However, the high velocities of SBCC 1 were confined to one side of an internal container thus providing space for lobsters to avoid excessively high velocities. Based on the assumption that lobsters will avoid high velocity by locating themselves in regions of low velocity, it can be implied that SBCC 1 at 90° AoA provided the best habitat at high input velocities.

4.3 Biofouling

The lower velocity limit performance of SBCC 1 at 90° AoA was not significantly affected by the percentage of biofouling. This implies SBCC 1 supplied enough DO after one-year deployment (66% biofouling) with 0.3 m/s input velocity. SBCC 2 struggled to supply enough DO when newly deployed (i.e. 0% biofouling) and this was exacerbated with biofouling; 66% biofouling resulted in 69% of measurements were below the lower velocity limit. Therefore, SBCC 2 was redesigned to increase X-axis flow through the container by increasing zones of mesh and changing the spacing between compartments.

4.4 Motion characteristics

The yaw motion results graded the SBCC containers against one another so an understanding of the severity of the physical movement was achieved. It showed that Oyster SBCC and SBCC 2 had stable yaw motions because the containers are circular with a central mooring point, thus no design changes are required from a motion stability perspective; however, SBCC 1 and 3 had unstable yaw motions and design improvements were required. SBCC 1 and 3 were unstable because they were designed to align with the flow direction. The cause of different motion severities between SBCC 1 at 0° AoA and 90° AoA was the length to width ratio. Hydrodynamic bodies are naturally unstable when the length to width ratio is less than one; this caused the harsher motion of SBCC 1 at 0° AoA. The external flow pattern visualisation results helped identify flow phenomenon, such as turbulent flow and separation points; therefore, methods could be recommended to reduce excessive yaw motion. Recommended methods included:

- Reposition the mooring point.
- Ensure length to width is greater than one.
- Trigger separation point at fixed location.
- Improve hydrodynamic shape of superstructure.

4.5 Normalised SBCC container comparison

Each performance criterion was normalised to allow a fair comparison between SBCC containers; see Appendix A. The normalised performances of individual criterion were combined to provide a normalised total score for each SBCC container (Fig. 21). The normalised comparison shows that SBCC 1 at 90° AoA (total score of 0.85) provides the best habitat for the survival and growth of lobsters, compared to the other containers tested in this study, due to good score against all performance criteria providing the lowest total score. The

next lowest total scores were provided by Oyster SBCC and SBCC 2. Advantages and disadvantages for Oyster SBCC and SBCC 2 can be seen from Fig. 21; outstanding performance in motion severity (score of 0 for both oyster SBCC and SBCC 2) but worst performance against the lowest velocity. Previous literature does not provide indication on the importance of one performance criterion against the other criteria; therefore, it is unclear whether all round good performance or outstanding performance related to one criterion would be preferable. Nonetheless, SBCC 1 at 90° AoA demonstrated all round performance as represented by the lowest normalised total score. Thus, based on the performance criteria considered in the present study, SBCC 1 is likely to provide the most suitable habitat for growth and survival of European lobster.

5 Conclusions

A systematic series of three hydrodynamic experiments were performed on novel SBCC containers to compare performance against known growth and survival criteria. Suitable graphical representations have been developed to assess SBCC containers and inform design decisions, for example design modifications were made to improve X-axis flow velocity in SBCC 2. Normalised comparisons were utilised to predict that SBCC 1 at 90° AoA will provide the most suitable habitat for growth and survival for European lobsters in relation the performance criteria assessed. In general, the circular Oyster SBCC container provided stable motion characteristics but insufficient exchange of fresh water; whereas, streamlined designs provide sufficient fresh water exchange but unstable motion characteristics. Further work would benefit from extending test parameters e.g. pitch AoA, waves or reducing input velocity below 0.1 m/s to investigate the laminar-turbulent transition. The current flume provides an idealised flow condition; therefore, the presented work will continue via full-scale sea trials in follow on project, Lobster Grower 2.

Acknowledgements

The research was gratefully supported and funded by BBSRC (BB/M005208/1) and Innovate UK (131597) through the Agri-Tech Catalyst, Early Stage Awards. The project consortium consisted of the National Lobster Hatchery, University of Exeter, Falmouth University, Centre for Environment, Fisheries and Aquaculture Science, West Country Mussels of Fowey and Fusion Marine. Follow on work will also be supported by BBSRC and Innovate UK through the Industrial Stage of Agri-Tech catalyst and supported by funding from the Worshipful Company of Fishmongers.

References

- Beal, B. F., Chapman, S. R., 2001. Methods for mass rearing stages I-IV larvae of the American lobster, *Homarus americanus* H. Milne Edwards, 1837, in static systems. *Journal of Shellfish Research*, 20(1), 337-346.
- Benavente, G. P., Uglem, I., Browne, R., Mariño Balsa, C., 2010. Culture of juvenile European lobster (*Homarus gammarus* L.) in submerged cages. *Aquaculture International*, 18, 1177-1189.
- Browne, R., Benavente, G. P., Mariño Balsa, C., Uglem, I., 2011. Lobster (*Homarus gammarus*). Stock enhancement in Ireland and collaborative efforts to improve postlarval on-growing techniques in sea cages without feed supplementation under an Aquareg Project (Interreg IIIc project) involving co-operation between Spain, Ireland and Norway.
- Burton, C. A., 2003. Lobster hatcheries and stocking programmes: an introductory manual. Sea Fish Industry Authority Aquaculture Development Service. Seafish Report, SR552.
- Daniels, C. L., Wills, B., Ruiz-Perez, M., Miles, E., Wilson, R. W., Boothroyd, D., 2015. Development of sea based container culture for rearing European lobster (*Homarus gammarus*) around South West England. *Aquaculture*, 448, 186-195.
- Davies, C.E., Whitten, M.M., Kim, A., Wootton, E.C., Maffeis, T.G., Tlusty, M., Vogan, C.L. and Rowley, A.F., 2014. A comparison of the structure of American (*Homarus americanus*) and European (*Homarus gammarus*) lobster cuticle with particular reference to shell disease susceptibility. *Journal of Invertebrate Pathology*, 117, 33-41.
- DESA, U.N., 2013. World population prospects: The 2012 revision. *Population Division of the Department of Economic and Social Affairs of the United Nations Secretariat*, New York.
- Drengstig, A., Bergheim, A., 2013. Commercial land-based farming of European lobster (*Homarus gammarus* L.) in recirculating aquaculture system (RAS) using a single cage approach. *Aquacultural Engineering*, 53, 14-18.
- Fox, J. A. 1977. *An introduction to engineering fluid mechanics*. Macmillan Press Ltd, second edition.
- Galparsoro, I., Borja, Á., Bald, J., Liria, P., Chust, G., 2009. Predicting suitable habitat for the European lobster (*Homarus gammarus*), on the Basque continental shelf (Bay of Biscay), using Ecological-Niche Factor Analysis. *Ecological Modelling*, 220, 556-567.
- Hamelø, J.S., 2006. Investigation of respiration rates of European lobster (*Homarus gammarus*) in land-based, lobster farming system. *Master Thesis*. Univ. of Stavanger, Norway, 86 p.
- Howard, A.E. and Nunny, R.S., 1983. Effects of near-bed current speeds on the distribution and behaviour of the lobster, *Homarus gammarus* (L.). *Journal of Experimental Marine Biology and Ecology*, 71(1), pp.27-42.

Jørstad, K.E., Prodöhl, P.A., Agnalt, A-L., Hughes, M., Farestveit, E., Ferguson, A.F., 2007. Comparison of genetic and morphological methods to detect the presence of American lobsters, *Homarus americanus* (H. Milne Edwards, 1837 (Astacidea: Nephropidae)), in Norwegian waters. *Hydrobiologia*, 590 (1), 103-114.

Nortek Vectrino Profiler, 2015. *Vectrino Profiler brochure*. Nortek AS, Vangkroken 1, 1351 Rud, Norway, 3 Nov. 2015 <<http://www.nortek-as.com/lib/brochures/vectrino-ii/view>>.

Mathiesen, A. M., 2012. The State of the World Fisheries and Aquaculture 2012.

Poindexter, C. M., Rusello, P.J., Variano, E.A., 2011. Acoustic Doppler velocimeter-induced acoustic streaming and its implications for measurement. *Experiments in Fluids* (50).

Rathakrishnan, E., 2007. Instrumentation, measurements and experiments in fluids. CRC Press.

Smith, I. P., Collins, K. J., Jensen, A. C., 1999. Seasonal changes in the level and diel pattern of activity in the European lobster *Homarus gammarus*. *Marine Ecology Progress Series*, 186, 255-264.

Stebbing, P., Johnson, P., Delahunty, A., Clark, P.F., McCollin, T., Hale, C. & Clark, S. (2012) Reports of American lobsters, *Homarus americanus* (H. Milne Edwards, 1837), in British waters. *BioInvasions Records*, 1(1), 17-23.

Sumer, B. M., Fredsøe, J., 2006. Hydrodynamics around cylindrical structures, 2nd edition (12) World Scientific.

Uglem, I., Benavente, G. P., Browne, R., 2006. A regional development strategy for stock enhancement of clawed lobsters (*Homarus gammarus*)-Development of juvenile lobster production methodologies. NINA Rapport 211: 39 pp., 211.

Van der Meeren, G.I., Ekeli, K.O., Jørstad, K.E. & Tveite, S., 2000. Americans on the wrong side - the lobster *Homarus americanus* in Norwegian waters. ICES Document CM 2000/U:20, 20, 1-15.

Van der Meeren, G.I., Støttrup, J., Ulmestrand, M., Øresland, V., Knutsen, J.A., Agnalt, A.-L. [Internet] NOBANIS Invasive Alien Species Fact Sheet: *Homarus americanus*. From: NOBANIS Online Database of the European Network on Invasive Alien Species. 2010. [Updated 06/02/2015; Accessed 01/09/2015] Available: https://www.nobanis.org/globalassets/speciesinfo/h/homarus-americanus/homarus_americanus.pdf

Dr Peter Halswell is a research fellow in the College of Engineering, Mathematics and Physical Sciences at the University of Exeter with a background of experimental research in hydrodynamics, structures, hydroelasticity and acoustics.



Dr Carly L. Daniels is the research and development officer at the National Lobster Hatchery, Padstow (UK), with a PhD in optimising the rearing diets of early life stages of the European lobster and has extensive experience in European lobsters culture via recirculated aquaculture systems and sea based container culture systems.



Professor Lars Johanning is the Professor of Ocean Technology in the College of Engineering, Mathematics and Physical Sciences at the University of Exeter and has been involved in research on hydrodynamic related topics for marine structures since 1997.

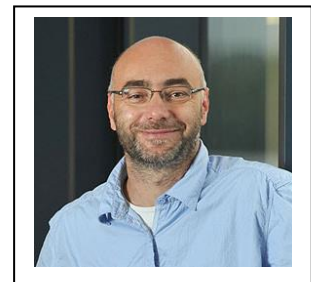


Figure captions

Fig. 1. (A) Stack of Oyster SBCC container tiers. (B) Individual compartments within a given tier.

Fig. 2. Diagrams of current flume: (A) Components of current flume; (B) Test section of current flume.

Fig. 3. Experimental setup: (A) computer model of model-bracket and end plates; (B) Model-bracket, end plates, sliding lid and Vectrino-Profiler.

Fig. 4. Oyster SBCC scale model.

Fig. 5. Example of 33% biofouling coverage.

Fig. 6. Vectrino-Profiler and traverse system: (A) Vectrino-Profiler and traverse; (B) Vectrino-Profiler probe head.

Fig. 7. Internal flow velocity measurement location in the Oyster SBCC at: (A) 0° AoA and (B) 36° AoA.

Fig. 8. Relationship between model-scale mean X-axis velocity and motor power of current flume with model-bracket installed, error bars show two standard deviations.

Fig. 9. Relationship between model-scale RMS turbulence velocity and motor power of current flume without model-bracket installed.

Fig. 10. 3D velocity magnitude of Oyster SBSS at 0.1 m/s input velocity along X-axis: (A) 0° AoA and (B) 36° AoA.

Fig. 11. 2D velocity and turbulent fluctuation of Oyster SBSS at 0.1 m/s input velocity along X-axis - 2D plane is 36 mm vertically above inner container floor: (A) 0° AoA and (B) 36° AoA.

Fig. 12. Cumulative histogram of X- and Y-axis velocity magnitude for Oyster SBCC at all input velocities and AoA (0.005 m/s bin size).

Fig. 13. Yaw motion visualisation of Oyster SBCC (viewing from underneath current flume; black marker lines represent internal containers).

Fig. 14. External flow visualisation of Oyster SBCC at 0.1 m/s input velocity and 0 cm release point; where (A) 0 s, (B) 7 s, (C) 13 s and (D) 22 s from start time.

Fig. 15. X-axis velocities cumulative histogram of all SBCC containers at 0.1 m/s input velocity (0.005 m/s bin size).

Fig. 16. Comparison of mean X-axis velocity against input velocity of all SBCC containers.

Fig. 17. X- and Y-axis velocities magnitude and turbulent fluctuation cumulative histogram of all SBCC containers at 0.5 m/s input velocity (0.005 m/s bin size).

Fig. 18. X-axis velocity cumulative histogram of SBCC 1 with biofouling at 0.3 m/s input velocity and 0° AoA (0.005 m/s bin size).

Fig. 19. X-axis velocity cumulative histogram of SBCC 2 with biofouling at 0.3 m/s input velocity and 0° AoA (0.005 m/s bin size).

Fig. 20. Measurement points that exceed the upper velocity limit in SBCC 2 at 0.7m/s input velocity along X-axis and 0° AoA (green marker indicate velocity < upper limit and red marker indicate velocity > upper limit).

Fig. 21. Total normalised comparison of SBCC containers (Table A.4).

Appendix A: Normalisation of performance criteria

Performance criteria values are normalised using the highest value of each performance criteria, thus lower scores indicate better habitat for growth and survival. Oyster SBCC and SBCC 2 are an average of both AoA because moored deployment angle could not be control in situ.

Table A.1

Normalisation of lower velocity limit.

SBCC	X-axis velocity (% < lower limit)	Norm.	Minimum input velocity (mm/s)	Norm.	Normalised score
Oyster	49.5	1.00	50	1.00	1.00
1 (0° AoA)	0.9	0.02	14	0.28	0.15
1 (90° AoA)	1.3	0.03	17	0.34	0.18
2	41.1	0.83	31.5	0.63	0.73
3	3.8	0.08	15	0.30	0.19

Table A.2

Normalisation of upper velocity limit at 0.7 m/s input velocity (*extrapolated).

SBCC	Velocity and RMS turbulent magnitude (% > upper limit)	Normalised score
Oyster	8.87*	0.10
1 (0° AoA)	85.8	0.97
1 (90° AoA)	70.4	0.80
2	30.4	0.34
3	88.5	1.00

Table A.3

Normalisation of motion severity.

SBCC	Magnitude of rotation (°)	Normalised score
Oyster	0	0
1 (0° AoA)	8.5	0.77
1 (90° AoA)	2.5	0.23
2	0	0
3	11	1.00

Table A.4

Normalised performance comparison.

SBCC	Lower velocity limit	Upper velocity limit	Motion severity	Total
Oyster	1.00	0.05	0.00	1.05
1 (0° AoA)	0.15	0.75	0.77	1.68
1 (90° AoA)	0.18	0.44	0.23	0.85
2	0.73	0.25	0.00	0.98
3	0.19	1.00	1.00	2.19